



Williams, S., Zhang, Q., De Kergariou, C. M. Y., & Scarpa, F. (2022). Investigating the Effect of Relative Humidity on the Mechanics and Dynamics of Open-Cell Polyurethane Auxetic Foams. *physica status solidi (b)*, 259(12), [2200442]. <https://doi.org/10.1002/pssb.202200442>

Publisher's PDF, also known as Version of record

License (if available):
CC BY

Link to published version (if available):
[10.1002/pssb.202200442](https://doi.org/10.1002/pssb.202200442)

[Link to publication record in Explore Bristol Research](#)
PDF-document

This is the final published version of the article (version of record). It first appeared online via Wiley at <https://doi.org/10.1002/pssb.202200442> . Please refer to any applicable terms of use of the publisher.

University of Bristol - Explore Bristol Research

General rights

This document is made available in accordance with publisher policies. Please cite only the published version using the reference above. Full terms of use are available: <http://www.bristol.ac.uk/red/research-policy/pure/user-guides/ebr-terms/>

Investigating the Effect of Relative Humidity on the Mechanics and Dynamics of Open-Cell Polyurethane Auxetic Foams

Samuel E. Williams, Qicheng Zhang,* Charles de Kergariou, and Fabrizio Scarpa

This work describes a series of investigations carried out on sets of pristine and auxetic (negative Poisson's ratio (NPR)) open-cell polyurethane foams subjected to relative humidity (RH) conditioning ranging from 9% to 92% at room temperature. The foams have been produced using a uniaxially thermoforming process. Pristine and auxetic foams have then been subjected to quasi-static compressive cyclic loading (with maximum strains of 10% and 80%, respectively), as well as vibration transmissibility tests with base accelerations up to 2.29 g. Increasing levels of RH do not seem to statistically affect the moduli and PRs of foams subjected to lower maximum strains, however, especially the auxetic foams at higher compressive deformations show a decrease in the stiffness with the increase of the RH. The vibration tests show an increasing trend of the dynamic modulus of the foams with the increase of the RH. The results indicate the complexity of the interaction between foam architecture and absorption/desorption mechanisms occurring inside these porous auxetic materials.

1. Introduction

During the past four decades, auxetics (i.e., negative Poisson's ratio (NPR)) materials and structures have been developed in different forms and scales, from molecular assemblies and nanostructures,^[1–8] metals systems,^[9–11] and lattices/perforations^[12–17] to multiphase composites.^[18–22] The reader is referred to the works of Alderson and Evans,^[23] Lakes,^[24,25] and Lim^[26,27] for an extensive review of morphologies and


performances of auxetic materials systems. Foams (both open and closed cells) are arguably one of the first and most successful materials products with auxetic characteristics, being described for the first time in Lakes' seminal article of 1987.^[28] Auxetic foams are mainly found in form of open-cell configurations, although techniques to transform closed-cell foams by steam and pressure do also exist.^[29–31] The most established manufacturing process to produce auxetic open-cell foams consists of a volumetric compression, annealing via heating, cooling, and relaxation.^[32–35] Volumetric compression creates the typical re-entrant cell structures of auxetic materials, while heating and cooling provide the thermoforming of the compressed foam, so that the shape of the re-entrant cell structures stabilizes after the foam is released

from compression. Other methods to replace the heating and cooling involve the use of compressed carbon dioxide^[36] or solvents.^[37] For more information about the aspects of manufacturing and characterizing auxetic foams, the reader is referred to the works of Critchley et al^[38] and Jiang et al.^[39] The triaxial volumetric compression is usually performed using customized molds involving lubrication by oil and manual compression of the foam, which makes large-scale productions difficult. A way to overcome this issue is to simplify the volumetric compression by compressing and thermoforming the foam in one direction only, albeit with some modifications to the temperature annealing profile.^[40,41] This approach has, however, advantages for applications in which relatively large mass-scale productions are required, like in sports equipment and biomedical (external) prosthesis.^[32,33] Low-frequency vibrations are also critical for the performance of vibration mat pads, or the use of foams as liners in anti-vibration gloves for machinery.^[42]

One of the environmental constraints of using open-cell foams in sports equipment, apparel, and prosthesis is their sensitivity toward humidity and moisture. With the close to body setting of personal protective equipment, it is reasonable to assume that foams would experience a high-humidity environment.^[43] It is also notionally known that the aging of open-cell polymeric foams is possible via exposure to varying relative humidity (RH) conditions.^[44] Transport properties of auxetic foams have been evaluated by Alderson, Rasburn, and Evans, however, their studies focused on pressure air drops and the way potential sieving effects were conditioned by the strain applied, the airflow

S. E. Williams, Q. Zhang, C. de Kergariou, F. Scarpa
Bristol Composites Institute
University of Bristol
University Walk, BS8 1TR Bristol, UK
E-mail: qicheng.zhang@bristol.ac.uk

S. E. Williams, F. Scarpa
Aerospace Engineering
School of Civil, Aerospace and Mechanical Engineering (CAME)
University of Bristol
BS8 1TR Bristol, UK

 The ORCID identification number(s) for the author(s) of this article can be found under <https://doi.org/10.1002/pssb.202200442>.

© 2022 The Authors. physica status solidi (b) basic solid state physics published by Wiley-VCH GmbH. This is an open access article under the terms of the Creative Commons Attribution License, which permits use, distribution and reproduction in any medium, provided the original work is properly cited.

DOI: 10.1002/pssb.202200442

rate, and the architecture of the foams used.^[45] Yet, little quantitative research investigating the effects of RH or moisture ingress on the mechanical performance of either auxetic or pristine open-cell PU foams is available in the open literature. Lapčik et al. have recently investigated the effect of thermal and humidity conditioning on pristine PU foams.^[46] Those authors found that conditioned foams became more compliant as the increased humidity caused the initiation of the degradation process. This shows the importance of similar testing on auxetic foams. It is even more important due to the open-cell nature of the foams being considered. This is because, unlike closed-cell foams whose gaseous pores are entirely encapsulated by the base material, the pores in open-cell foams are all connected in complex pore networks. The effect of moisture on the mechanical behavior of other auxetic metamaterials has also been evaluated analytically in refs. [47-49]. In those works, the moisture affects the mechanical properties of the metamaterials because of the embedding within the architectures of moisture-sensitive components.

If auxetic foams are to be commercially accepted for sports, apparel, and biomedical applications, manufacturers will need assurance that the performance witnessed under room conditions is still acceptable in specific application environments for which humidity and moisture absorption are different. The purpose of this work is to explore in quantitative terms the effect of varying levels of moisture on the mechanical properties (quasi-static and vibration-related) of both pristine and auxetic open-cell PU foams. The auxetic foams used in this work are produced using a relatively low-cost uniaxial thermoforming technique^[40] and conditioned at five different RH levels following procedures typical of porous composites, also with natural fiber reinforcements.^[50,51] The conditioned foams are subjected to quasi-static cyclic loading under large deformations, and vibration transmissibility tests following protocols already applied to foams at room temperature conditions.^[41,52] Tangent moduli, PRs, and quasi-static/dynamic loss factors have been measured, together with the dynamic modulus of those foams. Aging and effects on the static and dynamic properties of pristine and auxetic foams are discussed, together with the statistical significance of the data for future studies.

2. Experimental Section

2.1. Preparation of the Foam Samples

The open-cell polyurethane (PU) foam used for both the pristine and converted auxetic samples was sourced from SM Upholstery

Ltd. The density and pore linear density of this foam are 27.4 kg m^{-3} and $1102\text{--}1378 \text{ m}^{-1}$, respectively. The auxetic samples were manufactured using the conversion method developed in ref. [40]. The compression ratio used to create the auxetic samples was 60%, meaning that the height of the auxetic foam is 40% of that of the pristine foam before compression. After conversion, the samples were cut to dimensions of $30 \times 30 \times 15 \text{ mm}$ to satisfy the sizes set out in the American Polyurethane Association standard (ASTM D3574 CFD); however, it was not possible to satisfy the minimum dimensions due to the scale of the testing. The samples used in this work have been cut-oriented with the principal axis aligned with the d3 direction (**Figure 1a**). This alignment still results in samples with NPR effect.^[41] Moreover, it was noticed that the pristine samples had three clear groups with differing maximum stress and stress–strain curves, each relating to the direction in the loading was applied in relation to the rise direction of the foam.^[41] From 40 initial samples, a subset of 37 samples was found to produce similar mechanical responses and was therefore believed to have the same orientation with respect to the rise direction. The criterion used to select the 15 pristine samples evaluated in this work was the value of the interquartile range of the maximum stress, resulting in 18 eligible samples. As only 15 samples were required, the 15 closest to the mean and median values were chosen. Before the samples could be humidity conditioned, acrylic plates had to be bonded to the top and bottom of the specimens to provide an interfacing surface for the transmissibility testing rig used. These plates were $40 \times 40 \text{ mm}$, laser-cut from 3 mm acrylic plastic with an average mass of 5.387 g (grams). Samples were attached to the plates using Ever Build Industrial Superglue high viscosity (HV). The combined average mass added from gluing the top and bottom plates was 0.195 g per sample. To ensure that the samples were centered on the plates, $30 \times 30 \text{ mm}$ squares were laser engraved on the surface and jigs like that those shown in **Figure 1b** were used to align the top plate to the bottom. The samples were lightly pressed for 90 s for both the top and bottom plate attachment. **Table 1** shows the masses of the pristine and auxetic samples for each conditioning level, following plate attachment.

Small masses were placed on the samples overnight to ensure a strong bond.

2.2. RH Conditioning

The samples used in this work have been subjected to Indirect Conditioning, which consists in creating a specific RH

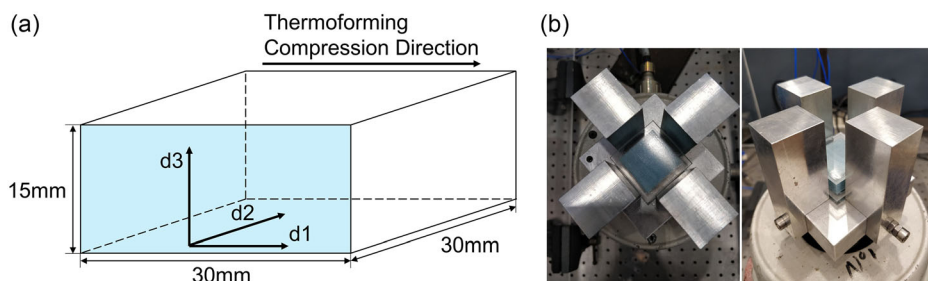


Figure 1. a) Orientation of the sample with respect to thermoforming direction and b) plate attachment and assembly jig.

Table 1. The masses of each sample (post plate bonding) before conditioning.

Auxetic samples					
Sample	Mass [g]	Sample	Mass [g]	Sample	Mass [g]
15% RH-1	11.725	34% RH-3	11.700	73% RH-2	11.782
15% RH-2	11.705	51% RH-1	11.670	73% RH-3	11.658
15% RH-3	11.672	51% RH-2	11.610	92% RH-1	12.030
34% RH-1	11.795	51% RH-3	12.070	92% RH-2	11.880
34% RH-2	11.915	73% RH-1	11.957	92% RH-3	11.735
Pristine samples					
Sample	Mass [g]	Sample	Mass [g]	Sample	Mass [g]
15% RH-1	11.356	34% RH-3	11.305	73% RH-2	11.291
15% RH-2	11.301	51% RH-1	11.316	73% RH-3	11.389
15% RH-3	11.422	51% RH-2	11.336	92% RH-1	11.293
34% RH-1	11.296	51% RH-3	11.361	92% RH-2	11.266
34% RH-2	11.324	73% RH-1	11.312	92% RH-3	11.373

environment within a conditioning chamber.^[53] One way of creating this type of environment is by using different salt solutions. Through careful selection of salts, a variety of RH can be achieved at different temperatures.^[54] The environment created by this indirect method is likely more representative of the environment that foams would face in the several potential applications. For this study, five RH conditioning levels were chosen with an expected RH range between 9% and 98% in the 20 °C room temperature lab. To achieve these RH values, the salt solutions used are those listed in **Table 2**. The PU foam has nominally a good/excellent resistance to those salts, although some disagreement still persists on HKO.^[55–57] It was decided to still use this salt, but with the condition that any diverging reaction would be noted if found. The spectrum of RH environments provided by the selected salts is each roughly separated by ±20%. The solutions were placed in airtight containers and samples were separated from the solutions via perforated acrylic stands.

Throughout conditioning, the RH of each box and the lab were measured using industry-standard humidity/temperature sensors. The reading of each of these sensors was recorded each time the boxes were opened, either to mass the samples or conduct testing. To ensure that the lab conditions were as consistent as possible for each recording, massing always took place between the hours of 8:30–10:00. This was important, as due

Table 2. Salts used for the RH conditioning and their predicted RH values.^[54]

Salt name	Chemical formula	Predicted humidity
Potassium hydroxide	HKO	9%
Magnesium chloride hexahydrate	Cl ₂ Mg · 6H ₂ O	33%
Magnesium nitrate hexahydrate	MgN ₂ O ₆ · 6H ₂ O	54%
Sodium chloride	NaCl	75%
Potassium sulphate	K ₂ O ₄ S	98%

to there being open-air ventilation, the lab conditions followed a loose day–night cycle. To recognize this cyclic hygrothermal behavior, only average values of temperature and RH are reported in this work. The change in mass of the samples was used as the main method of tracking the RH conditioning of the foam specimen. The samples were periodically massed every 72 to 96 h, using Ohaus Adventurer AR1530 scales (resolution of 0.001 g). This sample period was used, as it was found to have the lowest effect on the conditioning of the samples, whilst still providing sufficient data to track conditioning progression.

2.3. Quasi-Static Compression Testing

The samples have been subjected to quasi-static 10% strain cyclic (compression–compression) and 80% strain uniaxial compression tests. These tests were conducted on separate days to provide the samples time to regain some conditioning lost in the previous day's test. The 80% strain compression test results in partial softening of the samples, so this test was performed after the cyclic one. As all samples had undergone 80% compression case before the transmissibility test.

The setup used for these tests is shown in **Figure 2a**. The tests were conducted using a Shimadzu AGS-X test frame with a 1kN SSM-DAM load cell. It was found that a 1.5 and 3 N preload was required for the pristine and auxetic samples, respectively, to ensure that the top and bottom acrylic plates were parallel before testing commenced. After this preload was applied, the stroke and force were zeroed, to act as the initial state. Loading rates of ≈3 mm min^{−1} resulted in the recorded modulus of the foam being almost constant. This loading rate was used for the testing of these samples, instead of the 2 mm min^{−1} previously adopted,^[41] to reduce the time the samples were exposed to room conditions. It was indeed critical to reduce this exposure time, as it reverted the conditioning of the samples. Due to residual strains caused by the Mullins effect,^[58] there is poor agreement between the first few cycles of the 10% test, and therefore all post-processing and calculations are made with the data related to foams being tested at the 5th cycle.^[40,41] From the hysteretic loops, the tangent modulus E_t and the quasi-static loss factor $\eta_{C/T}$ were computed. The quasi-static loss factor of the compression test is the ratio of the energy dissipated per cycle ($\Delta W_{C/T}$) to the elastic energy stored by the sample ($U_{C/T}$) over the cycle^[52]

$$\eta_{C/T} = \frac{2\Delta W_{C/T}}{\pi U_{C/T}} \quad (1)$$

To capture the samples' strains along the lateral (ϵ_x) and longitudinal loading (ϵ_y) direction, a single-camera video gauge (VG) system (iMETRUM Limited, camera type MG146B PoE) was used. The locations of the tracking points are shown in **Figure 2b**. Two groups of strain measurement markers, each consisting of three sets of measurements in both the lateral and transverse, were used. The distance between the points was ≈30% and 70% of the length of the specimen for each respective group. This allowed for average values to be found and added redundancy to the measurements if markers lost their tracking points during the test. To reduce the chances of the VG

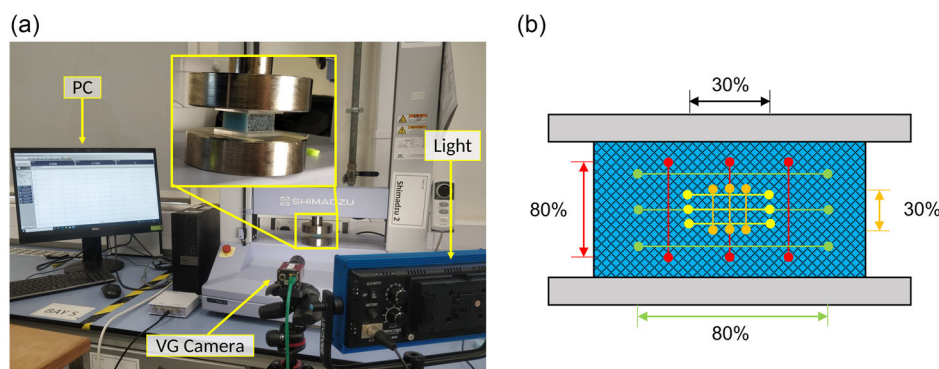


Figure 2. a) Compression testing rig and b) grid of measurement points in the foam samples.

losing the tracking regions, a cross-hatching pattern was also applied to the foam's face. This insured that there was an identifiable cross in each region, meaning that even when the foams deformed the VG could still locate the center of the cross. The engineering strains and stresses (also called nominal strains and stresses) are used for both the small (10%) and large strains (up to 80%) compression tests. According to previous observations made on open-cell foam materials under large compressive deformations,^[59] the PR calculated by using the nominal strains gradually reaches a maximum value at $\approx 20\%$ of strain, and then tends to approach 0 at large strains due to the densification of the porous foam material under larger compressions. Therefore, the change in the cross-section area of the foam samples at large compression strains does not appear to be significant and the use of the nominal stress would be acceptable within the context of this work. Ultimately, the values of PR were found using the 30% markers as these suffered less from the boundary effects and therefore produced more reliable results. To ensure that the samples were square to the camera and in the same place between tests, the tape was applied to the lower compression plate to create a tactile slot. These strains allowed the PR of the samples to be calculated as $\nu_{xy} = -\epsilon_y/\epsilon_x$. The foam used in this work is partially auxetic, showing NPR only when compressed within the transverse plane of the thermoforming direction.^[41] Partially auxetic properties have also been studied in crystal-type materials.^[60–62] Due to the anisotropic nature of the auxetic foams, the same face (d3–d1 face^[41]) was used for capturing the VG data from the auxetic foams.

2.4. Vibration Transmissibility

The procedure described in this paragraph shows the methodology previously used in ref. [52]. Low-amplitude white noise tests were conducted using an electrodynamic shaker (LDS, Model V406) to determine the effect of moisture on the energy absorption of the foams (Figure 3a). Two (PCB, Model 333M07) accelerometers were used to record the difference between the accelerations of the base and top plates. These tests took place 1 week after the compression testing to allow for the foams' moisture levels (i.e., mass) to be comparable to the levels seen before the quasi-static compression test had been conducted.

As previously discussed, acrylic plates were bonded to the foam samples with superglue before conditioning. These plates provided an interfacing surface to the dynamic rig. Double-sided tape was used to attach the samples to the rig. For consistency, the direction in which the tape was applied was the same for each sample. To minimize the risk of the top mass rocking during the test, the jig seen in Figure 3b was used again to ensure that samples were bonded to the center of the base plate and that the top mass system was placed directly on top of the sample. The samples were all oriented with the crosshatched (d3–d1 face) facing in the same direction, (Figure 3a). This was precautionary so that, in the case that the rocking of the top mass occurred, the sample would have the same directional properties interacting with the rocking.

A range of four masses were used to vary the load on the sample during the tests. The testing was conducted over 2 days, with

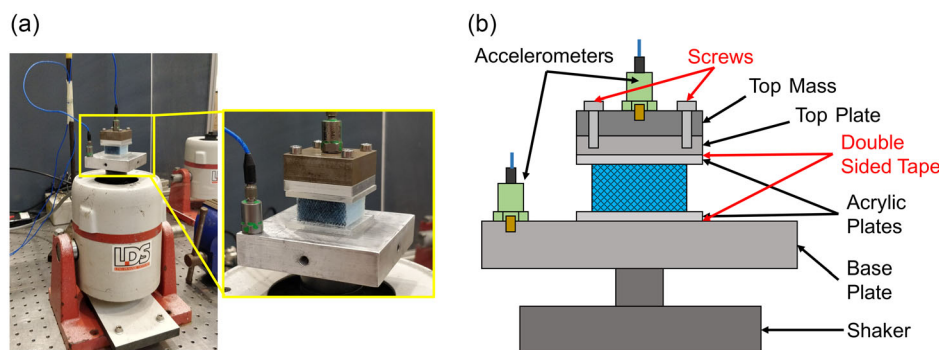


Figure 3. a) Vibration transmissibility rig and b) schematics of the component of the rig.

two mass cases being tested each day. To minimize the amount of moisture lost before the second test, the following scheme was selected. On the first day, the M1 case was tested, followed directly by the M3 one. Similarly, the M2 case was tested before the M4 one on the second day. By having the lightest mass tested first on each day, it was believed the moisture levels would be as similar as possible to the start level of that day. The different masses and the accelerometers were attached using screws (see Figure 3b). The combined masses for each test case, which includes the accelerometer, top acrylic plate, double-sided tape, top plate, top mass, and screw masses, are outlined in **Table 3**. The same scales as mentioned earlier were used, except for the top mass in the M4 case. For this mass, Kern EMB2200 scales (resolution 1 g) were used as the mass exceeded the 150 g limit in the previous scales.

The test protocol involved two cycles of white noise tests which were generated using a MATLAB code. Each cycle consisted of 10 s of white noise at five constant, but each time increased energy levels, resulting in a total cycle time of 50 s. The root mean square (RMS) acceleration applied to the base plate associated with each energy level was: 4.6, 7.6, 12.0, 17.9, and 22.5 ms⁻². There is a 10 s rest period between the first and second test to allow the foam to settle. Only the samples' responses to the second white noise cycle were used for the interpretation of the data.

To supply the analog signal required to actuate the shaker, the digital output of the MATLAB code was passed through an NI USB-6211 module and then amplified using an LDS PA100E power amplifier, with a setting of 4, before reaching the shaker. The same MATLAB code was also used to collect and store the outputs of the systems, so an NI 9234 module was needed to digitalize the accelerometers' analog output.

From the output of the accelerometers, the transmissibility function (TF) of the sample can be found as the ratio between the output (top) and input (base) in the frequency domain. The maximum amplitude of the TF occurs at the resonant frequency ω_R related to the point of maximum amplitude of the TF for each sample and the corresponding 180° phase change. Identification of these values is represented in **Figure 4**. From the resonant frequency and the know masses of both the sample (m) and top mass case (M) tested, the dynamic stiffness (k_d) and dynamic modulus (E_d) can be found using Equation (2) and (3),^[52] respectively

$$k_d = \omega_R^2 \left(M + \frac{m}{3} \right) \quad (2)$$

$$E_d = \frac{k_d A}{H} \quad (3)$$

Table 3. Types of masses used for the vibration transmissibility tests.

Mass case	Mass [g]
M1	70.112
M2	116.975
M3	166.29
M4	215.288

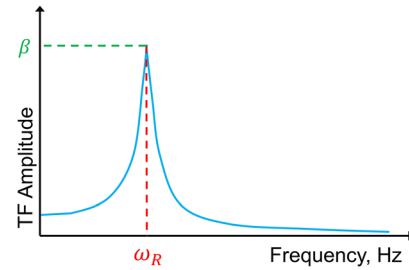


Figure 4. Representative parameters for a vibration transmissibility test.

If damping is assumed to be small,^[52] the dynamic loss factor η_d can be calculated using Equation (4), where β is the amplitude of the TF at resonance

$$\eta_d = \frac{M + \frac{m}{2}}{M + \frac{m}{3}} \frac{1}{\sqrt{\beta^2 - 1}} \quad (4)$$

2.5. Statistical Treatment of the Data

In this work, Chauvenet's Criterion^[63] has been used to identify potential outlying samples within the RH groups. The criterion measures the deviation of the tested sample (x_i) from its group's mean (\bar{x}) using the following relationship: deviation = $|x_i - \bar{x}|/s$, where s is the standard deviation of the samples within that group. Due to the properties of the pristine foams being quite consistent between the different batches, it has been assumed that the responses of the pristine samples tested here are representative of a small sample of a wider population. Therefore, Equation (5) can be used to calculate the standard deviation.

$$s = \sqrt{\frac{\sum (x_i - \bar{x})^2}{(n - 1)}} \quad (5)$$

Variability within auxetics foams manufactured from the same batch of pristine foam and the same conversion method^[40,41] of pristine foam leads to consider the auxetic specimens as being the whole population, so Equation (6) is used instead^[64]

$$s = \sqrt{\frac{\sum (x_i - \bar{x})^2}{n}} \quad (6)$$

A sample is deemed to be an outlier if its deviation is greater than a critical value. When testing between samples from the same RH condition (three samples), the critical value is 1.383, while when testing whether an RH group has deviated from the rest or not, the critical value is 1.645.^[64] Although five samples would have been used at each RH instead, as commonly used for composite materials (ASTM D3039/D3039M-08), this was not possible due to the lack of available foams. Therefore, within this article, any potential outliers identified by Chauvenet's Criterion will be discussed, but their results will not be removed from further discussions.

3. Results and Discussion

3.1. RH Conditioning

The achieved RH level of each conditioning box compared to the expected one is shown in **Table 4**. In each case, the actual RH recorded does not exactly match the predicted RH level. This is due to multiple causes. When predicting these values, it was assumed that the average lab temperature was 20 °C, however, during testing the temperature of the laboratory was found to be 18.6 °C. Furthermore, the day/night temperature cycle that occurred in the laboratory could imply that the actual average temperature of the boxes was different from that measured between 9:00 and 10:30. The discrepancies between the predicted and actual RH levels are, however, relatively small and range between 3% and 4%, except for the 66% of the RH = 9% predicted level.

The change in mass of the samples was used to track the progress of the samples' conditioning. These mass readings were taken every 72–96 h. This period minimized the frequency that the boxes' lids were opened, which resulted in large humidity gradients and changes in the boxes RH values. **Figure 5a,b** shows the average change in mass of the samples from each humidity level, with time expressed in days. Both auxetic and pristine foams appear to acquire similar levels of mass after ≈18–20 days at 51% and 72% RH levels. The mass of the foam specimens is virtually stable at 34% RH, with a slight decrease over time for the 15% RH. The error bars show the maximum and minimum mass values from the three samples at each RH level. Both pristine and auxetic samples separate into five distinct groups, with a

regular separation like that between the actual RH values. The two groups of foams show a degree of plateauing with the time of exposure to the RH levels; this is more significant for the auxetic specimens.

Conditioning of the samples was conducted over 18 days and 36 days for the pristine and auxetic samples, respectively. The auxetic samples started conditioning before the pristine foams, as it was assumed that the more complex pore network and the higher tortuosity of the auxetic samples^[45,65,66] would lead to a slower conditioning rate. To provide more comparable responses between the foams, the pristine samples were subjected to the conditioning later, with the aim that both foams would have a similar final conditioning for testing. This assumption was proven to be correct, as after 10 days the average change of the pristine samples' mass was greater than the one seen in the auxetic samples at the same RH level after 11 days. At the start of testing, however, the auxetic samples at extreme RH values were conditioned slightly more than the pristine ones, but the samples belonging to the central RH levels (34%, 51%, and 73%) were more similar. The only major difference between the two cases was the 34% RH case. In the auxetic samples, there was a net decrease in mass over its conditioning period. Conversely, the pristine samples seemed to show little change, with only 0.003 g increase in mass before testing began. This would suggest that when the auxetic samples entered the conditioning chamber, they were at a higher initial RH level than 34%, resulting in their decreased mass. The slight change observed in the pristine samples suggests that those specimens were close to the 34% RH level, when their conditioning commenced. Traditionally, samples are dried in an oven before testing to ensure that all samples start from the same conditions.^[53] However, drying in the oven was avoided to not trigger possible reconversion of the foams due to their shape memory effect.^[67] The large positive error bars seen in **Figure 5a,b** for the 92% RH samples were both due to the #3 sample of each type of foam (auxetic and pristine). As the other two samples at this humidity showed a better agreement with each other, there is ground to believe that the position of these samples within the conditioning boxes was a potential cause of this. These samples were closer to the window, compared to the other samples closer to the front of the box. This could have led to a different temperature toward this end, causing a minor convection current. With this high

Table 4. Predicted and achieved RH levels.

Salt name	Predicted humidity	Achieved humidity
Potassium hydroxide	9%	15%
Magnesium chloride hexahydrate	33%	34%
Magnesium nitrate hexahydrate	54%	51%
Sodium chloride	75%	73%
Potassium sulfate	98%	92%

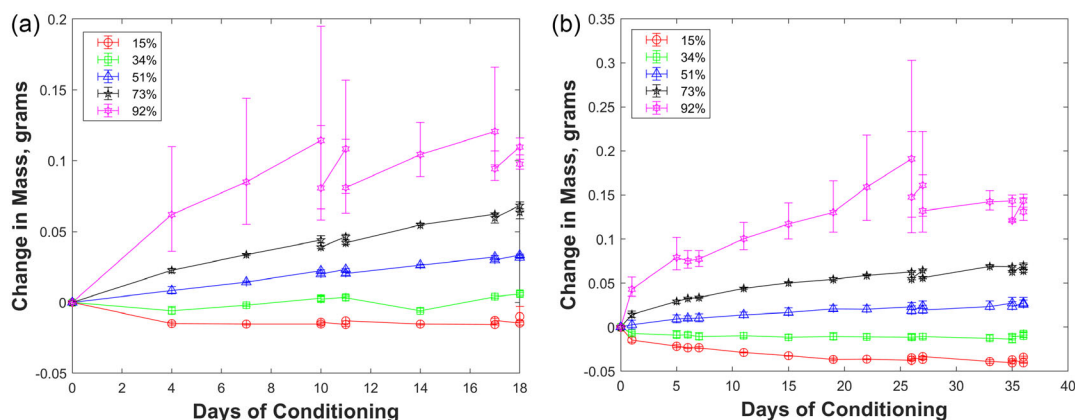


Figure 5. Changes of mass of the: a) pristine and b) auxetic samples with the periods of conditioning for the different relative humidity (RH) levels.

humidity, large water droplets are being formed on the wall and lids of the boxes. Before massing, water droplets sometimes had to be wiped off the acrylic plates, before to avoid misrecording the mass. It is possible that some of these droplets may have contacted the foam causing direct moisture absorption. Chauvenet's Criterion is applied to both the change in mass between each reading, and the change compared to the initial mass for each reading. The auxetic sample fails the test, but the deviation of the pristine sample was found to be less than the critical value (maximum deviation of 1.412 and 1.155, respectively). Due to the comments made earlier regarding the validity of applying the population standard deviation to the auxetic samples, this potential outlying sample was not disregarded from the testing. Also, the error bars of the samples reduce after testing begins. Before testing, the positive error bar was 59% greater than the average value, but only 9% on day 33 and reducing further after the transmissibility test. This may suggest that the excess moisture was lost during testing. After the 80% compression test, the auxetic sample's deviation no longer fails Chauvenet's Criterion, meaning that the samples would not be deemed outliers for the transmissibility test that followed.

3.2. Quasi-Static Compression

Figure 6a,b shows a representative response of auxetic and pristine samples to the 10% and 80% strain quasi-static compression tests, respectively. In Figure 6a, the max strain shown is 8%, despite the test being conducted with 10% strain. This difference is due to the residual strain, which causes the start and end of the fifth cycle to occur at $\approx 2\%$ strain. In the figure, the residual has been removed and the curves have been shifted to the origin. The auxetic foam is stiffer than the pristine one, with the maximum stress of the auxetic foam being 89.9% larger for the 10% compression ratio, and 414% larger for the 80% compression case. This stiffening effect provided by the conversion of a foam into an auxetic phase has also been witnessed previously, as well as in other papers where a comparison between auxetic and pristine response has been made. Figure 6c,d also shows the mean maximum stress of the samples at 7% and 70% strain for each RH of both the pristine and auxetic samples, from the 10% and 80% tests, respectively. Although there is no significant trend shown in the pristine foams-related data, the auxetic foams, especially those at the 80% test, seem to have a mild trend of decreased

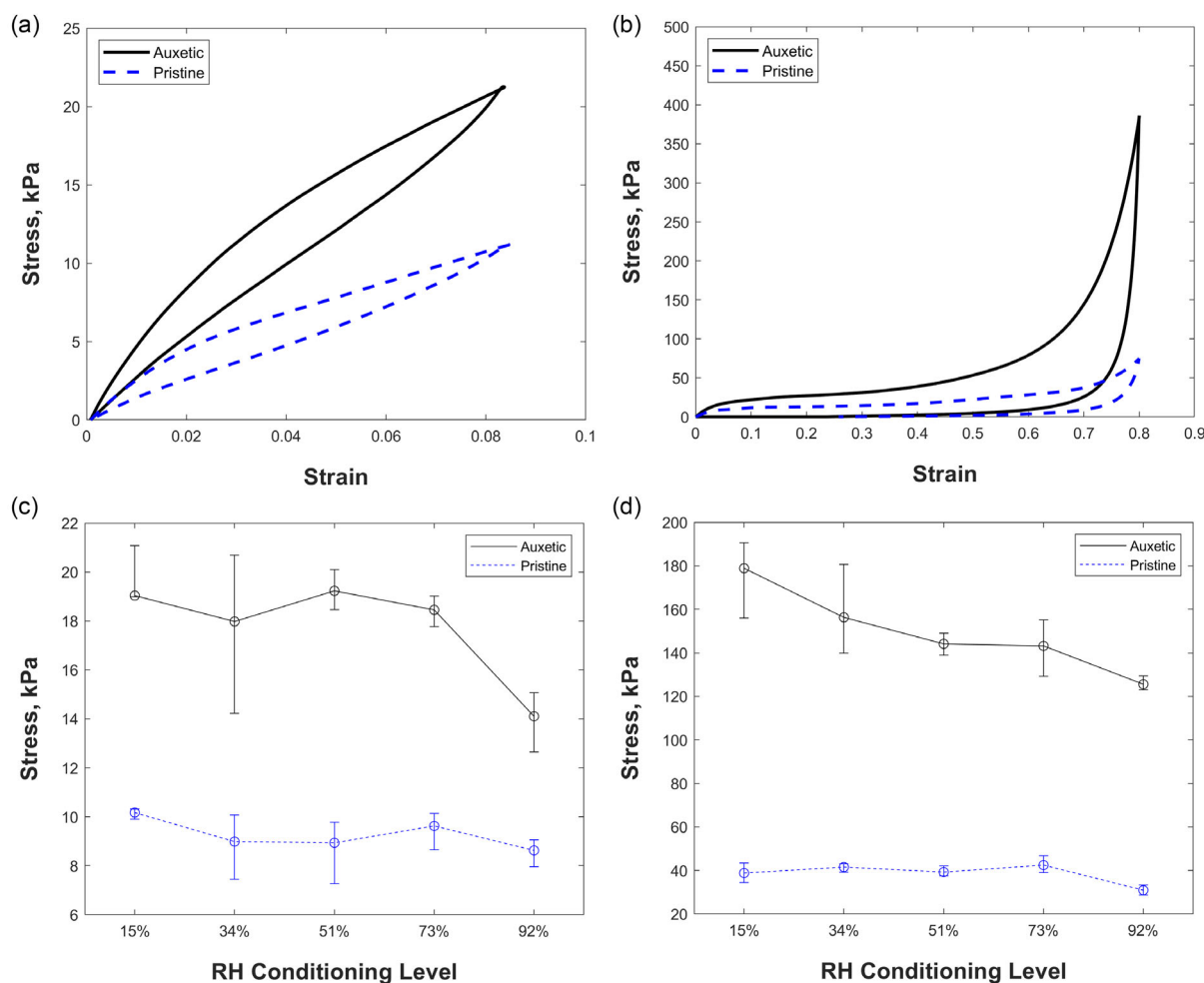


Figure 6. Representative responses of the pristine and auxetic samples for both the: a) 10% and b) 80% strain compression tests. The bottom plots show the mean values related to each RH each level (pristine and auxetic) at: c) 7% on the 10% strain test, and d) 70% on the 80% strain test.

maximum stress with increasing humidity. This could suggest that increased moisture has the effect of softening the foams at low loading rates.

As alluded to aforementioned, the residual strain in the samples resulted in the foams not starting their fifth cycle from the origin. After eliminating the residual strains, the minimum–maximum strain reached by one sample was 7.6%. The 7% value was, therefore, chosen to provide an offset from the tip of the lowest curve. Similarly, 70% was chosen to provide an offset from the maximum 80% strain.

The average tangent modulus, E_t , of each RH value for the pristine and auxetic samples seems to split into two clear groups (Figure 7a,c). The auxetic samples are all grouped, except those with the highest RH values at 92%, which consistently tracks below the other samples at a near-constant separation. This is not as clear in the pristine samples, due to the average responses of the 34% and 51% RH samples also grouping with the 92% RH ones. On closer inspection, the negative error bars of the 34% RH and 51% RH are large and become progressively larger as the strain increases. These error bars are caused by the number 1 (N1) samples in the respective RHs. After looking at the stress-strain responses of these samples, the author believes that these samples may have had their orientation, with respect to rise direction, misidentified. The test outlined in the methodology

was believed to give reliable identification, but the responses of these samples are clearly different from the rest of the population. They also have a near-identical agreement with each other. If these samples were removed from the calculation of the mean response shown in Figure 7a, the same grouping would be shown as that seen in the auxetic samples. Furthermore, the strong agreement between the 34% and 51% RH auxetic samples shows that those N1 samples may suggest to be potential outliers. However, Chauvenet’s Criterion applied to those samples shows that neither of them exceeds the critical value of 1.383, with both having deviations of ≈ 1.155 . This would suggest that these samples are not outliers. As the samples are suspected of having a different orientation to the other tested, Chauvenet’s Criterion was used against all the pristine samples, also. This causes both samples to fail with deviations of ≈ 3 which are far greater than the critical value of 2.128 (for a 15-sample test).^[64] This would suggest that these two samples do belong to a different orientation group than the rest of the other pristine samples tested. This reiterates why all potential outliers found in this work are only commented on, as the statistical test from three samples did not identify these as an outlier when the large sample size test did. Moreover, if these N1 samples are true outliers, then the highest humidity samples would again be alone tracking a similar trend as the other samples, but at a constantly lower value of tangent

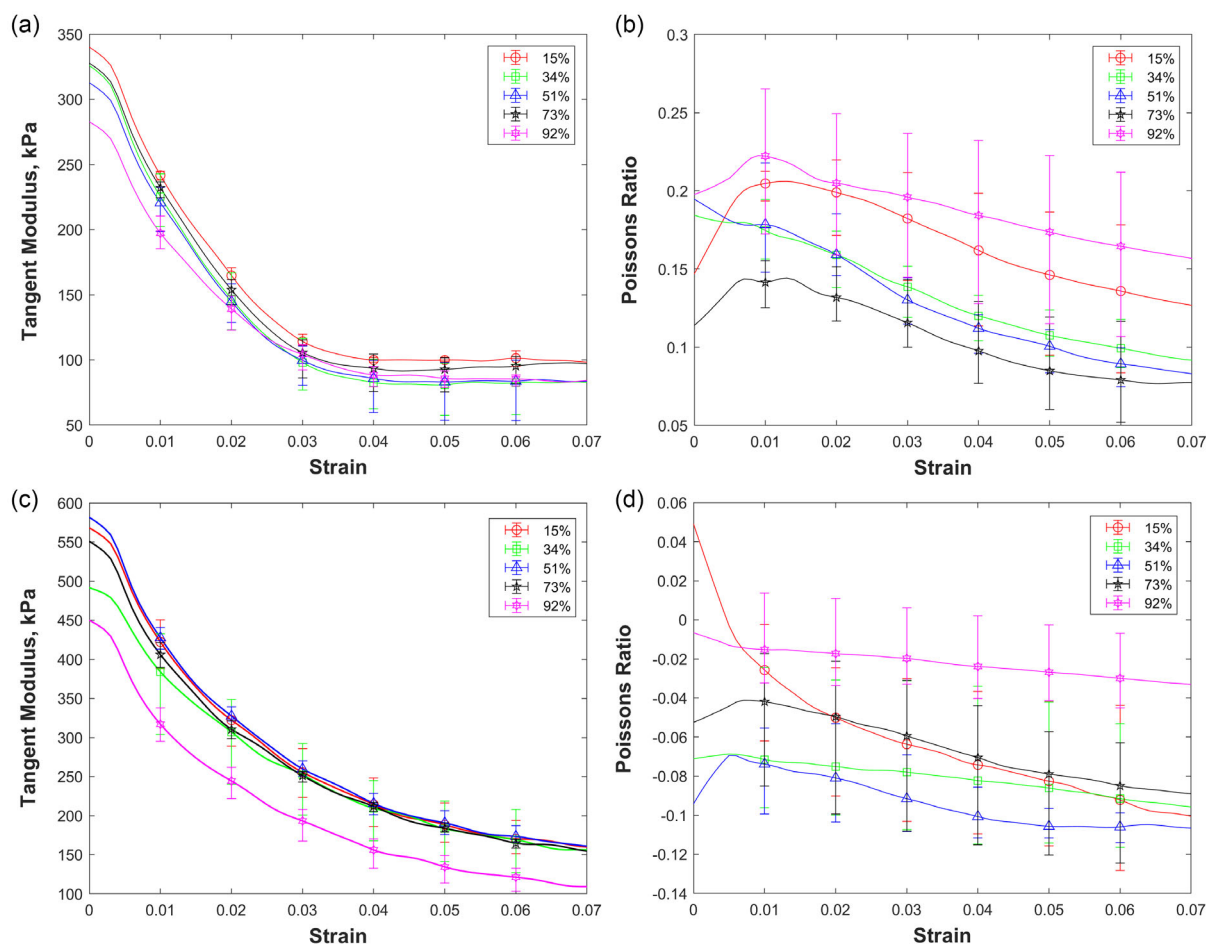


Figure 7. Tangent Modulus and PR against strain, up to 7% strain for the: a,b) pristine and c,d) auxetic samples at varying RH levels.

modulus compared to the other specimens. This could suggest that exposure to high humidity could degrade the foam, resulting in a softer response. Lapčík et al. have indeed found that increased humidity causes initiation of degradation.^[46]

Like the tangent modulus, the PR shown in Figure 7d of both the 92% RH pristine and auxetic samples seem to be separated from the other specimens, despite the 15% RH pristine samples making this separation less obvious (Figure 7b). All values of the PR for the pristine samples are positive and the auxetic samples all show an NPR for most of the strain range. The 15% RH samples are the only nominally auxetic samples to have a non-NPR at small strains. This is partially caused by slack and unstable contact between the compression plate and the sample. Unlike the tangent modulus, each RH's samples seem to have a different PR curve. The general trend of the pristine samples is a rise in PR until the 1% strain value, for which the PR begins to steadily decrease, so that the PR at 7% is below the one near the zero strain. This same distribution can be observed for the 51% and 73% RH auxetic samples. The 15% and 92% auxetic foams seem to initially decrease like those belonging to the 34% and 51% RH groups. After a 2% strain value, the auxetic samples appear to similarly show a steady decrease in PR with increased strain, similar to what has been observed in the pristine samples.

Figure 8a,b summarizes the values of the tangent modulus, PRs, and loss factors at 7% strain for each RH value considered. Both pristine and auxetic foams show similar trends in terms of mechanical response to the different humidity levels. The samples conditioned at 92% RH show, however, a different behavior and divergence from the other specimens. The Chauvenet's Criterion applied to the auxetic samples at 92% RH samples fail for both the PR and tangent modulus showing that those specimens may be statistical outliers. The pristine foam cases pass the criterion; however, PR has a divergence of 1.499, which is close to the critical value of 1.645. This suggests that with a slightly less conservative statistical test, the RH could also seem to deviate from the mean response. The loss factor of the auxetic samples is consistently below that of the pristine samples (Figure 8b). This is consistent with previous on identical and unconditioned samples.^[40,41] If the N1 samples from the 34% and 51% RHs were classed as outliers as earlier, the agreement between the trends of the auxetic and pristine samples would be strong, as

in Figure 8a. This is because those samples are the cause of the large positive error bars observed in the respective RH conditions.

3.3. Vibration Transmissibility

Figure 9a shows a representative transfer function (TF) curve for both the auxetic and pristine samples. The resonant frequency of the auxetic foam is higher than that of the pristine, but both seem to have a similar maximum TF amplitude. The specific foam samples used in these graphs are the number 2 (N2) conditioned at 51% RH. The top mass used was the M2 case (117.0 g). Figure 9b shows the TF curves of the auxetic 51% RH N2 samples for each mass case considered. With increasing top mass, the resonant frequency of the system reduces, but the maximum TF amplitude shows little variation. This shows that the increased gravity load does not affect the damping performance of the foams, for the range of masses tested. This is a trend that is seen observed across samples from all RH values considered, and in the pristine samples too. The spikes present in higher frequencies of the phase response are most likely due to the numerical rounding when wrapping the phase response. Their presence is not considered further.

All the base acceleration levels used in this work produced a similar response for each sample-mass configuration. However, the 5th base acceleration level (22.5 ms^{-2} , corresponding to 2.29 g) sometimes caused a response with a slightly flattened peak. This type of transfer function is indicative of the potential presence of small misalignments of the center of mass of the sample in relation to the axis in which the dynamic load was being applied. This slight offset would have led to a slight rocking of the top mass for these samples, with a nonlinear mass/pendulum effect. The 12.0 ms^{-1} case was therefore chosen for the overall assessment of the behavior of the foams in the rest of this section, due to its good agreement with the other base acceleration levels.

The effect of the varying top mass cases and RH levels on the resonant frequencies of the foams can be seen in Figure 10a,b. The small error bars show consistency between the different samples. Both the pristine and auxetic specimens exhibit a steady

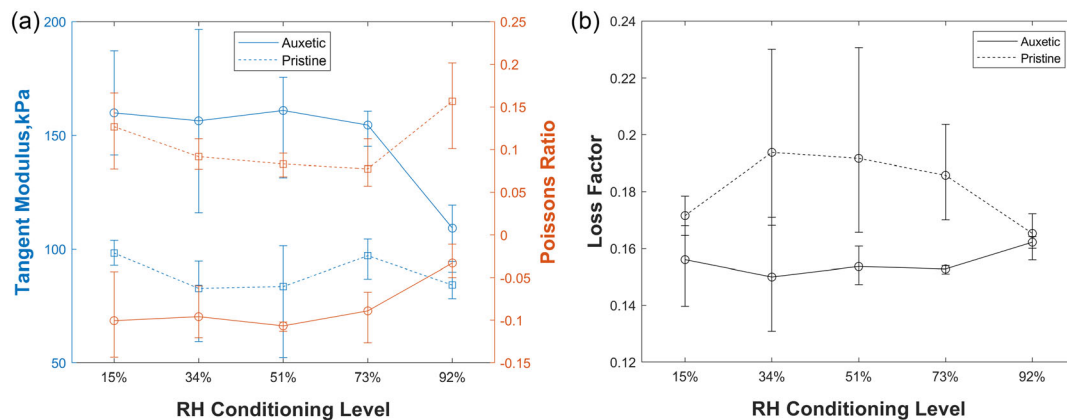


Figure 8. a) Average values of the tangent modulus and PRs at each RH level for the pristine and auxetic samples at 7% strain. b) Average loss factors for the same samples.

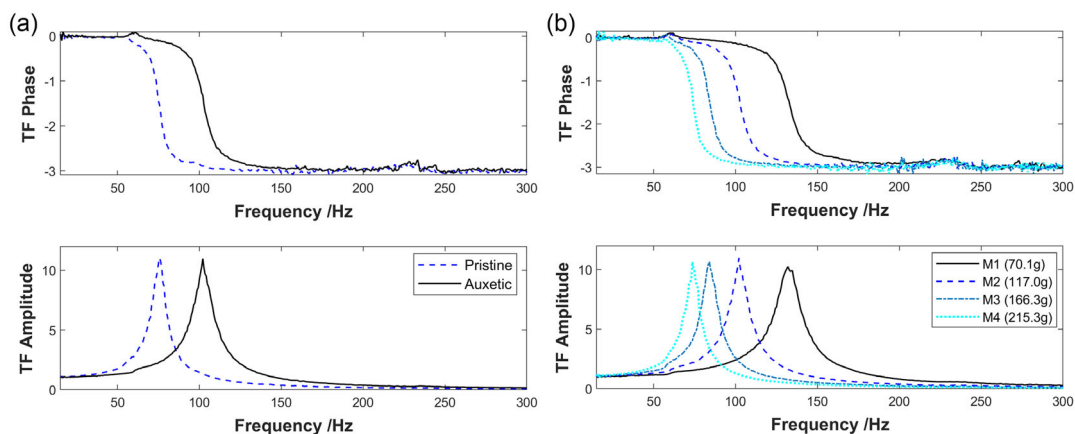


Figure 9. a) Comparison of transmissibility responses from representative auxetic and pristine samples. b) The effect of varying the top mass.

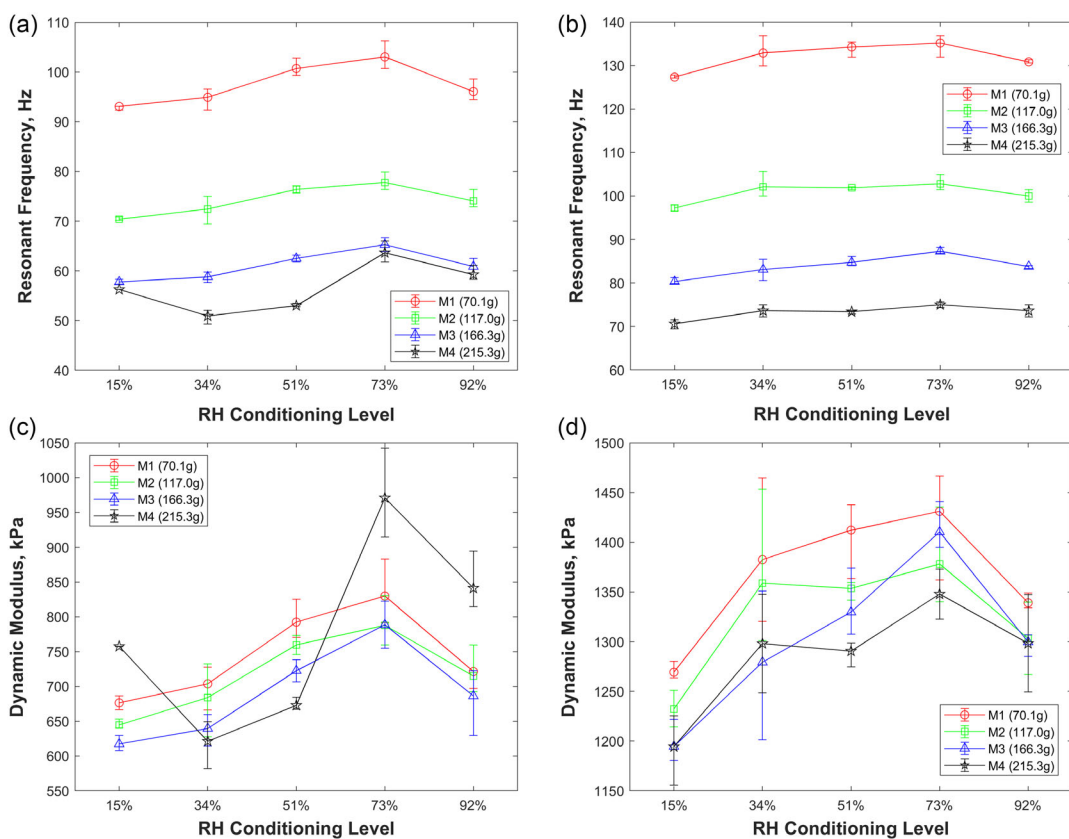


Figure 10. Trends of key parameters obtained from the vibration transmissibility tests of the samples against each RH level. a) Resonant frequency and c) dynamic modulus of the pristine foam; b) Resonant frequency and d) dynamic modulus of the auxetic foam.

increase in resonant frequency, as the RH value increases. On average, the 73% RH conditioned samples have a resonant frequency 7 Hz higher than the 15% RH samples, across all mass cases. Again, the trend does not stay true for the highest humidity case (92%); in this case, it falls by 4 Hz on average compared to the 73% RH-conditioned specimens. This again hints at a potential aging effect present in the foams from the highest

humidity level, first suggested in relation to the tangent modulus response of these samples.

It is important to note the change in the size of the error bars related to the dynamic modulus extracted from Equation (3) and shown in Figure 10c,d, compared to the resonant frequency in Figure 10a,b. The different mass cases have less of an effect on the dynamic modulus, resulting in a closer range of responses.

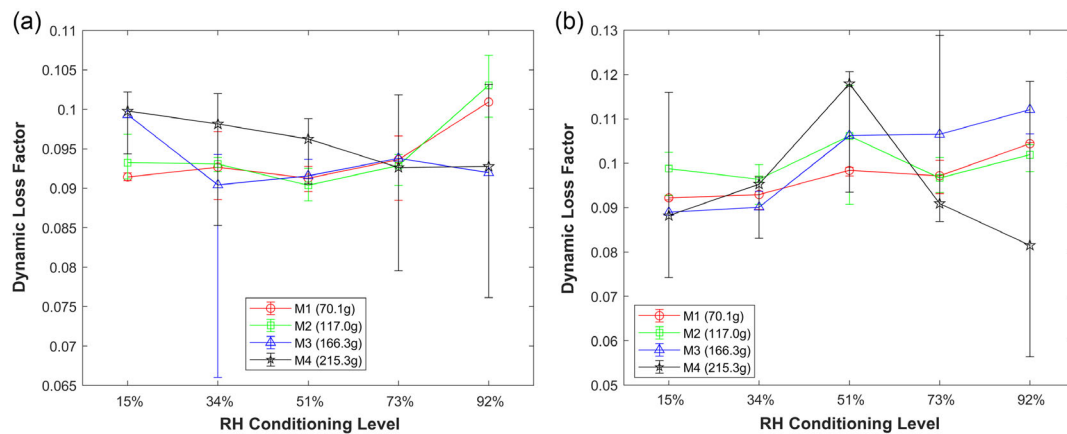


Figure 11. Dynamic loss factors of the: a) pristine and b) auxetic samples.

This smaller range has the effect of enlarging the error bars and made the sensitivity of the dynamic modulus versus the RH levels more prominent. A potential cause of this relationship may be the incompressibility of water. Unlike the quasi-static compression testing where the loading was slow, steady, and continuous, the sudden and everchanging compression and tension cycles provided by the dynamic loading may have led to the movement of the moisture within the pore network becoming more difficult. Also, in some cases, it may have led to some moisture becoming trapped within the pores. With increasing moisture levels, it would be expected that this problem would become more prevalent, as more moisture could get trapped and impede the movement of other moisture. The trapping or increased difficulty in the movement of moisture would lead to a stiffening effect, like the one observed in liquid-saturated foams.^[44] This was likely not seen in the quasi-static compression as the slow steady loading meant that the moisture could more easily flow through the microstructure of the foams. The dynamic moduli found here are all larger than those found during the compression tests by an average of 126% for the pristine and 162% for the auxetic foams. A similar trend was found in transmissibility tests on uniaxially thermoformed auxetic foams; however, those results only saw a 40% and an 82–98% increase for the pristine and auxetic foams respectively.^[52] The presence of moisture content, therefore, appears to increase the pneumatic stiffening generated by the poroelastic effect due to the resistivity and kinematic viscosity of the air trapped in the foam.^[52] This may also explain the greater difference between the dynamic and tangent moduli found within the specimens tested in this work and those on similar samples tested under loading, but unconditioned.

Figure 11a,b shows the dynamic loss factors calculated using Equation (4). There is no obvious trend between each RH level present in both the auxetic and pristine foams, with the dynamic loss factors all clustered around 0.095. The dynamic loss factors we find here are lower than the quasi-static loss factors found by the compression testing by an average of 0.07. It must be pointed out that no obvious trend between compression ratios and dynamic loss factors in unconditioned foams was already observed in ref. [52], with loss factors clustered between 8%

and 13% in that case—both for the pristine and the auxetic foams.

4. Conclusion

In this work, 30 open-cell PU foam specimens were conditioned to 5 distinct humidity levels. Fifteen of those samples belonged to a new type of uniaxially thermoformed open-cell PU auxetic foams, while the remnants were the pristine counterparts. The RH levels achieved in the chambers were: 15%, 34%, 51%, 73%, and 92%. The samples showed leveling off the moisture desorption, with masses sufficiently separated. Auxetic samples were found to be stiffer than their pristine counterparts, something that was also seen observed in previous works. No obvious trend relating to varying humidity was identified for the cyclic 10% strain test; however, there was some evidence of decreased maximum stress with increased humidity found from the auxetic foams made from an 80% compression ratio. Specimens conditioned at 92% of RH showed, however, different types of mechanical response, suggesting possible rapid aging or degradation of the open-cell foams when exposed to high humidity levels for a prolonged period. Dynamic white noise vibration transmissibility testing of the samples found a noticeable increase in resonant frequency and dynamic modulus with increasing levels of humidity. Similar to the results from the compression tests, this trend was not, however, obeyed by the 92% RH conditioned samples. In both quasi-static cyclic and vibration test schemes, the loss factors of the samples showed, however, no obvious trend versus the RH, with the compressive loss factors found to average around 16% and the dynamic ones around 9.5%.

This work has also shown the need to perform tests with a larger number of samples per repeat when RH conditioning is required. Two potential outliers were identified in the pristine foam samples, but due to the small population size, their responses we not removed, just commented on. Questions also on the behavior of auxetic foams with larger NPR values versus the RH conditioning also arise; the foam samples tested here had PRs with marginally zero values, with a minimum of -0.1 . The results shown in this work are, however, indicative of the

presence of complex interactions between moisture absorption, the microstructure of the auxetic foams, and their mechanical response to both static and dynamic loading. With microstructures and morphology of auxetic foams significantly dependent upon the different manufacturing processes used, the understanding of how they behave in different environmental conditions may be critical for their use and selection of production processes.

Acknowledgements

The project has been supported by the UK Engineering and Physical Sciences Research Council (EPSRC) EP/R032793/1 SYSDYMATs. F.S. also acknowledges the support of the ERC-2020-AdG 101020715 NEUROMETA project. The authors would also like to thank the anonymous reviewers for the suggestions and constructive comments.

Conflict of Interest

The authors declare no conflict of interest.

Data Availability Statement

The data that support the findings of this study are available from the corresponding author upon reasonable request.

Keywords

auxetic foams, environmental conditioning, mechanical tests, relative humidity, vibration

Received: September 14, 2022

Revised: October 17, 2022

Published online: November 8, 2022

- [1] K. W. Wojciechowski, A. C. Brańka, *Phys. Rev. A* **1989**, 40, 7222.
- [2] J. N. Grima, S. Winczewski, L. Mizzi, M. C. Grech, R. Cauchi, R. Gatt, D. Attard, K. W. Wojciechowski, J. Rybicki, *Adv. Mater.* **2015**, 27, 1455.
- [3] D. T. Ho, V. H. Ho, H. S. Park, S. Y. Kim, *Phys. Status Solidi B* **2017**, 254, 1700285.
- [4] J. W. Narojczyk, K. W. Wojciechowski, *Phys. Status Solidi B* **2008**, 245, 2463.
- [5] J. W. Narojczyk, K. W. Wojciechowski, K. V. Tretiakov, J. Smardzewski, F. Scarpa, P. M. Pigłowski, M. Kowalik, A. R. Imre, M. Bilski, *Phys. Status Solidi B* **2019**, 256, 1800611.
- [6] J. W. Narojczyk, K. V. Tretiakov, K. W. Wojciechowski, *Phys. Status Solidi B* **2022**, 259, 2200006.
- [7] K. E. Evans, M. A. Nkansah, I. J. Hutchinson, S. C. Rogers, *Nature* **1991**, 353, 124.
- [8] K. W. Wojciechowski, *Phys. Lett. A* **1989**, 137, 60.
- [9] V. V. Krasavin, A. V. Krasavin, *Phys. Status Solidi B* **2014**, 251, 2314.
- [10] D. T. Ho, S.-D. Park, S.-Y. Kwon, T.-S. Han, S. Y. Kim, *Phys. Status Solidi B* **2016**, 253, 1288.
- [11] D. S. Lisovenko, J. A. Baimova, L. K. Rysaeva, V. A. Gorodtsov, A. I. Rudskoy, S. V. Dmitriev, *Phys. Status Solidi B* **2016**, 253, 1295.
- [12] F. Sun, C. Lai, H. Fan, D. Fang, *Mech. Mater.* **2016**, 97, 164.
- [13] Y. Li, Y. Chen, T. Li, S. Cao, L. Wang, *Compos. Struct.* **2018**, 189, 586.
- [14] L. Mizzi, D. Attard, K. E. Evans, R. Gatt, J. N. Grima, *Acta Mech.* **2021**, 232, 779.
- [15] J. N. Grima, R. Gatt, *Adv. Eng. Mater.* **2010**, 12, 460.
- [16] J. N. Grima, L. Mizzi, K. M. Azzopardi, R. Gatt, *Adv. Mater.* **2016**, 28, 385.
- [17] L. Mizzi, D. Attard, R. Gatt, A. A. Pozniak, K. W. Wojciechowski, J. N. Grima, *Composites B: Eng.* **2015**, 80, 84.
- [18] J. N. Grima, L. Oliveri, B. Ellul, R. Gatt, D. Attard, G. Cicala, G. Recca, *Phys. Status Solidi RRL* **2010**, 4, 133.
- [19] C. T. Herakovich, *J. Compos. Mater.* **1984**, 18, 447.
- [20] K. L. Alderson, V. R. Simkins, V. L. Coenen, P. J. Davies, A. Alderson, K. E. Evans, *Phys. Status Solidi B* **2005**, 242, 509.
- [21] C. P. Chen, R. S. Lakes, *J. Mater. Sci.* **1993**, 28, 4288.
- [22] A. A. Poźniak, K. W. Wojciechowski, J. N. Grima, L. Mizzi, *Composites B: Eng.* **2016**, 94, 379.
- [23] K. E. Evans, A. Alderson, *Adv. Mater.* **2000**, 12, 617.
- [24] R. Lakes, *Adv. Mater.* **1993**, 5, 293.
- [25] R. Lakes, *Composites and Metamaterials*, World Scientific, Singapore **2020**.
- [26] T.-C. Lim, *Auxetic Materials and Structures*, Springer Singapore, Singapore **2015**.
- [27] T.-C. Lim, *Mechanics of Metamaterials with Negative Parameters*, Springer, New York **2020**.
- [28] R. Lakes, *Science* **1987**, 235, 1038.
- [29] E. O. Martz, T. Lee, R. S. Lakes, V. K. Goel, J. Park, *Cell. Polym.* **1996**, 15, 229.
- [30] N. Li, Z. Liu, X. Shi, D. Fan, H. Xing, J. Qiu, M. Li, T. Tang, *Adv. Eng. Mater.* **2022**, 24, 2100859.
- [31] O. Duncan, G. Leslie, S. Moyle, D. Sawtell, T. Allen, *Smart Mater. Struct.* **2022**, 31, 074002.
- [32] K. Alderson, A. Alderson, N. Ravirala, V. Simkins, P. Davies, *Phys. Status Solidi B* **2012**, 249, 1315.
- [33] T. Allen, T. Hewage, C. Newton-Mann, W. Wang, O. Duncan, A. Alderson, *Phys. Status Solidi B* **2017**, 254, 1700596.
- [34] O. Duncan, F. Clegg, A. Essa, A. M. T. Bell, L. Foster, T. Allen, A. Alderson, *Phys. Status Solidi B* **2019**, 256, 1800393.
- [35] R. Critchley, V. Smy, I. Corni, J. A. Wharton, F. C. Walsh, R. J. K. Wood, K. R. Stokes, *Sci. Rep.* **2020**, 10, 18301.
- [36] Y. Li, C. Zeng, *Adv. Mater.* **2016**, 28, 2822.
- [37] J. N. Grima, D. Attard, R. Gatt, R. N. Cassar, *Adv. Eng. Mater.* **2009**, 11, 533.
- [38] R. Critchley, I. Corni, J. A. Wharton, F. C. Walsh, R. J. K. Wood, K. R. Stokes, *Phys. Status Solidi B* **2013**, 250, 1963.
- [39] W. Jiang, X. Ren, S. L. Wang, X. G. Zhang, X. Y. Zhang, C. Luo, Y. M. Xie, F. Scarpa, A. Alderson, K. E. Evans, *Composites B: Eng.* **2022**, 235, 109733.
- [40] Q. Zhang, W. Lu, F. Scarpa, D. Barton, K. Rankin, Y. Zhu, Z.-Q. Lang, H.-X. Peng, *Mater. Des.* **2021**, 211, 110139.
- [41] Q. Zhang, X. Yu, F. Scarpa, D. Barton, K. Rankin, Z.-Q. Lang, D. Zhang, *Composites B: Eng.* **2022**, 237, 109849.
- [42] ISO 5349-1 Standard, **2001**.
- [43] P. J. Sullivan, I. B. Mekjavić, *Aviat. Space Environ. Med.* **1992**, 63, 186.
- [44] L. J. Gibson, M. F. Ashby, *Cellular Solids: Structure and Properties*, 2nd edn, Cambridge Press, Cambridge, UK **1997**.
- [45] A. Alderson, J. Rasburn, K. E. Evans, *Phys. Status Solidi B* **2007**, 244, 817.
- [46] L. V. Lapčík, M. Vašina, B. Lapčíková, Y. Murtaja, *Materials* **2022**, 15, 195.
- [47] T.-C. Lim, *Phys. Status Solidi B* **2021**, 258, 2100137.
- [48] M. N. M. Allam, A. F. Radwan, M. Sobhy, *Eng. Struct.* **2022**, 251, 113433.
- [49] M. H. Mansouri, M. Shariyat, *Composites B: Eng.* **2015**, 83, 88.
- [50] C. de Kergariou, A. Le Duigou, V. Popineau, V. Gager, A. Kervoelen, A. Perriam, H. Saidani-Scott, G. Allegri, T. H. Panzera, F. Scarpa, *Composites A: Appl. Sci. Manuf.* **2021**, 141, 106183.

- [51] C. de Kergariou, H. Saidani-Scott, A. Perriman, F. Scarpa, A. Le Duigou, *Composites A: Appl. Sci. Manuf.* **2022**, 155, 106805.
- [52] Q. Zhang, X. Yu, F. Scarpa, D. Barton, Y. Zhu, Z.-Q. Lang, D. Zhang, *Mech. Syst. Signal Process.* **2022**, 179, 109375.
- [53] Y.-J. Yu, K. Hearon, T. S. Wilson, D. J. Maitland, *Smart Mater. Struct.* **2011**, 20, 085010.
- [54] L. Greenspan, *J. Res. Natl. Bur. Stand. A: Phys. Chem.* **1977**, 81A, 89.
- [55] Chemical Resistance of Polyurethane Foams, <https://gcpat.com/en/solutions/products/chemical-resistance-polyurethane-foams> (accessed: April 2022).
- [56] P. Resins, Common Chemical Resistance Chart For Polyurethane Foams Rating Code, <https://www.primeresins.com/media/3756/common-chemical-resistance-chart.pdf> (accessed: April 2022).
- [57] Cole-Parmer, Chemical Compatibility Database, <https://www.coleparmer.com/chemical-resistance> (accessed: April 2022).
- [58] R. W. Ogden, D. G. Roxburgh, *Proc. Roy. Soc. Lond. A: Math. Phys. Eng. Sci.* **1999**, 455, 2861.
- [59] Q. Zhang, F. Scarpa, D. Barton, Y. Zhu, Z.-Q. Lang, D. Zhang, H.-X. Peng, *Int. J. Impact Eng.* **2022**, 163, 104176.
- [60] A. C. Brańka, D. M. Heyes, K. W. Wojciechowski, *Physica Status Solidi B* **2009**, 246, 2063.
- [61] K. V. Tretiakov, K. W. Wojciechowski, *Phys. Status Solidi RRL* **2020**, 14, 2000198.
- [62] K. V. Tretiakov, K. W. Wojciechowski, *Phys. Status Solidi RRL* **2022**, <https://doi.org/10.1002/pssr.202200288>.
- [63] J. R. Taylor, *An Introduction to Error Analysis: The Study of Uncertainties in Physical Measurements*, 2nd edn., University Sciences Books, New York **1997**.
- [64] Zach, Chauvenet's Criterion: Definition & Example, <https://www.statology.org/chauvenets-criterion/> (accessed: April 2022).
- [65] F. Scarpa, L. G. Ciffo, J. R. Yates, *Smart Mater. Struct.* **2003**, 13, 49.
- [66] J. Paulose, B. G. Chen, V. Vitelli, *Nat. Phys.* **2015**, 11, 153.
- [67] M. Bianchi, F. Scarpa, C. W. Smith, *Acta Mater.* **2010**, 58, 858.